ANTIMICROBIAL AGENTS AND CHEMOTHERAPY, Oct. 2011, p. 4631–4638 Vol. 55, No. 10
0066-4804/11/$12.00 doi:10.1128/AAC.00650-11

Development of Peptide-Conjugated Morpholino Oligomers as Pan-Arenavirus Inhibitors▽†

Benjamin W. Neuman,[1] Lydia H. Bederka,[2] David A. Stein,[3] Joey P. C. Ting,[4] Hong M. Moulton,[5] and Michael J. Buchmeier[2]*

University of Reading, Reading RG6 6AJ, United Kingdom[1]; The University of California, Irvine, California[2]; Vaccine and Gene Therapy Institute, Oregon Health and Science University, Beaverton, Oregon[3]; Lilly Biotechnology Center, San Diego, California[4]; and Oregon State University, Corvallis, Oregon[5]

Received 11 May 2011/Returned for modification 1 July 2011/Accepted 20 July 2011

Members of the *Arenaviridae* family are a threat to public health and can cause meningitis and hemorrhagic fever, and yet treatment options remain limited by a lack of effective antivirals. In this study, we found that peptide-conjugated phosphorodiamidate morpholino oligomers (PPMO) complementary to viral genomic RNA were effective in reducing arenavirus replication in cell cultures and *in vivo*. PPMO complementary to the Junín virus genome were designed to interfere with viral RNA synthesis or translation or both. However, only PPMO designed to potentially interfere with translation were effective in reducing virus replication. PPMO complementary to sequences that are highly conserved across the arenaviruses and located at the 5′ termini of both genomic segments were effective against Junín virus, Tacaribe virus, Pichinde virus, and lymphocytic choriomeningitis virus (LCMV)-infected cell cultures and suppressed viral titers in the livers of LCMV-infected mice. These results suggest that arenavirus 5′ genomic termini represent promising targets for pan-arenavirus antiviral therapeutic development.

Most arenaviruses are carried by a single species of rodent host (reviewed in reference 5). In these rodents, arenaviruses have a unique life cycle characterized by benign and persistent infection. Arenavirus infections of humans, however, may cause serious illness. Arenaviruses are typically divided into Old World viruses, which are prevalent in Africa, and New World viruses, for which the Americas are the area of endemicity. Lassa virus, an Old World arenavirus, is a significant public health problem, primarily in West Africa, causing 300,000 to 500,000 cases of Lassa fever and approximately 5,000 deaths annually (21). Several New World arenaviruses, including Junín virus, Machupo virus, and Guanarito virus, can cause potentially deadly hemorrhagic fever syndromes in humans and occur epidemiologically as outbreaks, usually in South America (5).

No highly effective antiviral therapeutic against arenavirus infection is approved for use in humans. Intravenous treatment with ribavirin early after the onset of Lassa fever is effective in reducing mortality (13) but ineffective in preventing neurological sequelae, including deafness (16). The only approved prophylactic against arenavirus infection is an attenuated Candid#1 strain of the New World Junín virus, which has been used to vaccinate people in areas of endemicity against Argentine hemorrhagic fever but is generally unavailable elsewhere (15).

The unusual process of arenavirus gene expression may offer several opportunities for therapeutic intervention. All arenaviruses have a single-stranded, ambisense RNA genome containing two segments, "L" and "S," each of which encodes two proteins. The "L" segment encodes polymerase (L) and matrix (Z) protein and the "S" segment nucleoprotein (NP) and glycoprotein (GPC). All arenaviruses contain nearly identical complementary sequences at the 5′ and 3′ termini of each genomic segment (4). Although the exact replication initiation mechanism has yet to be fully clarified, the "S" segment requires a panhandle structure formed by these complementary 5′ and 3′ genomic termini for RNA synthesis (23). Studies using Tacaribe virus have provided evidence for a nontemplate nucleotide incorporation at the 5′ genomic terminus for viral RNA replication to yield a novel "prime and realign" mechanism for replication initiation (11, 12, 26).

Arenavirus proteins are expressed from subgenomic mRNAs that contain a 5′ cap structure and untemplated nucleotides at the 5′ end but lack 3′ polyadenylation. It has been proposed that a highly stable intergenic RNA stem-loop structure, present within each transcript, functionally compensates for the lack of 3′ polyadenylation (17, 24). NP and L are expressed from subgenomic mRNA transcripts that are transcribed from full-length packaged virion RNA (vRNA) segments, whereas Z and GP are expressed from subgenomic mRNA transcripts produced as nascent complements of full-length packaged virion RNA (vcRNA) segments (5).

In an attempt to develop inhibitors of arenavirus infections, we designed antisense phosphorodiamidate morpholino oligomers (PMO) with activity against several regions of viral genetic sequence considered important to arenavirus gene expression. PMO are single-strand nucleic acid analogs composed of uncharged phosphorodiamidate linkages connecting six-member morpholine ring subunits to which any nitrogenous base may be attached. PMO are uncharged, nuclease-resistant compounds that bind their target RNA sequence via Watson-

* Corresponding author. Mailing address: Molecular Biology and Biochemistry, University of California, Irvine, 3205 McGaugh Hall, Irvine, CA 92697-3900. Phone: (949) 824-5781. Fax: (949) 824-9437. E-mail: m.buchmeier@uci.edu.

† Supplemental material for this article may be found at http://aac.asm.org/.

▽ Published ahead of print on 8 August 2011.

TABLE 1. PPMO sequences used in this study

PPMO	5′–3′ sequence[a]	Position (in bases)[b]	Strand[c]
TERM-L	R-CGCCTAGGATCCCCGGTGCG	1–20	L vRNA
TERM-L-REP	R-CGCCTAGGATCCCCGGTGCGC	1–20[d]	L vRNA
TERM-S	R-GCCTAGGATCCACTGTGCGC	1–19[d]	S vRNA
3′TERM-L	R-CGCACCGGGGATCCTAGGCG	7095–7114	L vRNA
3′TERM-S	R-CGCACAGTGGATCCTAGGCA	3394–3413	S vRNA
AUG-GP	R-TAATGAACTGCCCCATTGTGC	81–101	S vRNA
AUG-NP	R-ATGCCAGAAGTTCTGGTGATT	3327–3348	S vcRNA
AUG-Z	R-TGCCCATTTGTCTGCCTCTTC	70–90	L vRNA
AUG-L	R-GATTCCTCCATGCTCAAGTGC	7074–7094	L vcRNA
IGS-S	R-CCTCCCCAGTCCGCGGCCAG	1609–1628	S vRNA
RANDOM	R-AGTCTCGACTTGCTACCTCA		

[a] All sequences included a 5′-conjugated $(RXR)_4XB$ peptide (R) that mediates delivery.
[b] Nucleotide positions on vcRNA are numbered as the corresponding bases of the vRNA based on GenBank AY746353 and AY746354.
[c] The entries in column 4 represent the presence of segment L or S followed by the sense that matches that of the target sequence.
[d] These PPMO include one additional 3′-terminal nucleotide that can base pair with the nontemplated 5′ G residue that is found on intracellular viral RNA template strands.

Crick base pairing and inhibit gene expression through a steric blockade (30, 34). Conjugation of an arginine-rich cell-penetrating peptide to the 5′ end of a PMO, to produce peptide PMO (PPMO), has been shown to greatly enhance cellular uptake (1, 10, 18). PPMO designed for activity against the genetic material of numerous RNA viruses have shown considerable antiviral activity *in vitro* and *in vivo* (reviewed in reference 31).

Here, PPMO was tested for activity against four distantly related arenaviruses: lymphocytic choriomeningitis virus (LCMV), Pichinde virus (PICV), Tacaribe virus (TCRV), and Junín virus (JUNV) strain Candid#1. LCMV, an Old World arenavirus, is used as a model for the more dangerous Lassa virus; PICV is closely related to the North American hemorrhagic fever agent Whitewater Arroyo virus, and TCRV clusters phylogenetically with the South American hemorrhagic fever viruses Machupo virus and JUNV. Together, these viruses cover the breadth of pathogenic human arenaviruses. We report that PPMO targeting the conserved 5′-terminal region of the viral genomic segments were effective at inhibiting viral protein expression and reducing viral titers in cell cultures and in LCMV-infected mice.

MATERIALS AND METHODS

Cells and viruses. JUNV Candid#1, LCMV Arm53b, TCRV, and PICV were grown in Vero-E6 cells as previously described (19). Vero-E6 cells were maintained in Dulbecco's minimal essential medium (DMEM) supplemented with 10% fetal bovine serum, 1% penicillin-streptomycin, 5 mM L-glutamine, and 10 mM HEPES buffer. For experiments using PPMO, cell cultures were maintained in serum-free medium (VP-SFM; Invitrogen) supplemented with 1% penicillin-streptomycin and 5 mM L-glutamine. Arenaviruses were titrated by plaque assays using Vero-E6 cells as previously described for LCMV (6).

PPMO synthesis. PMO were synthesized as previously described (35) and covalently conjugated to an arginine-rich cell-penetrating peptide of the composition $(RXR)_4XB$ (in which X stands for 6-amino hexanoic acid and B stands for beta-alanine) as previously described (1) to produce PPMO. All PPMO were produced at AVI BioPharma Inc. (Corvallis, OR).

Bioinformatics. The viral RNA sequences used to design PPMO are shown in Table 1 and were derived from sequences with the following GenBank accession numbers: AY746353 and AY746354 (JUNV Candid#1), NC_006439 and NC_006447 (PICV), NC_004291 and NC_004294 (LCMV), and NC_004292 and NC_004293 (TCRV). Pathogenic JUNV sequences which were also used in PPMO design included strains Rumero (AY619640 and AY619641) and XJ13 (NC_005080 and NC_005081). BLAST-n (NCBI) was used to establish that these sequences were representative of their type species, and ClustalW2 was used to align sequences.

Evaluation of PPMO toxicity for cell cultures and for mice. The cytotoxicity of PPMO was evaluated under conditions designed to mirror those of the antiviral assays described below. Briefly, Vero E6 cells were plated onto 6-well plates and incubated with VP-SFM (Invitrogen) supplemented with antibiotic-antimycotic (Gibco) and L-glutamine. Increasing concentrations of PPMO were added to the cells, and PPMO were allowed to incubate for 24 h. After 24 h or 96 h of incubation, 200 μl of MTT [3-(4,5-dimethyl-2-thiazolyl)-2,5-diphenyl-2H-tetrazolium bromide] (Sigma) (5 mg/ml) was added to each well and plates were allowed to incubate for an additional 40 min. Supernatant was removed, cells were solubilized with 1 ml of dimethyl sulfoxide (DMSO), and absorbance at 560 nm was measured using a Victor^3 plate reader (Perkin Elmer).

C57/Bl6 mice were used for all experiments. Mice were purchased from The Jackson Laboratory (Bar Harbor, ME) and housed at The Scripps Research Institute (La Jolla, CA). The mice were 6 to 8 weeks old at the beginning of the experiments. Mice were allowed food and water *ad libitum* throughout the studies, and all experimental procedures were preapproved and performed according to the guidelines set by the SRI Animal Care and Use Committee. *In vivo* toxicity testing was performed by injecting uninfected male mice intraperitoneally with PPMO or sterile saline solution. Experimental animals were treated with TERM-L, TERM-S, or TERM-L-REP PPMO (one dose containing ~9 mg/kg of body weight per mouse per day), and treatment continued for 5 days. At the conclusion of the experiment, mice were humanely euthanized and sections of liver and kidney were stained with hematoxylin and eosin. Samples were randomized and relabeled for observations performed in a blinded manner. Samples were examined using a light microscope for signs of chromatin degradation or other histopathologic changes.

PPMO treatment and viral infection of cell cultures. Vero-E6 cells in T25 culture flasks were treated with PPMO in 2 ml of VP-SFM and incubated for 3 h prior to inoculation. Cells were inoculated at an approximate multiplicity of infection (MOI) of 0.01. Inoculum was then added to the treatment medium and removed after a 1-h adsorption period. The cells were then rinsed once with phosphate-buffered saline (PBS), and fresh VP-SFM containing the appropriate dose of PPMO was readded. Cell supernatant and cell lysates were collected at various time points, starting at 24 h postinoculation. For cytoprotection assays, cells were fixed with neutral buffered formalin at 96 h after inoculation, stained with crystal violet, and evaluated using a light microscope.

Western immunoblot analysis. To obtain cell lysates, LCMV-infected Vero E6 monolayers were incubated for 10 min in 1× PBS–1 mM EDTA and then harvested by centrifugation and subjected to titration in 1% NP-40 lysis buffer (20 mM Tris [pH 7.6], 140 mM NaCl, 5 mM $MgCl_2$) containing a 1× protease inhibitor cocktail (RPI Corp.). Protein concentrations in cell lysates were determined using a standard BCA kit and the manufacturer's protocol. Samples were separated using 12% Tris-glycine gels under reducing conditions, and proteins were transferred to nitrocellulose membranes. Membranes were blocked with buffer containing 5% milk protein, probed overnight with monoclonal antibodies (MAb) targeting the GP2 region of either the LCMV glycoprotein (MAb 83.6) or the LCMV nucleoprotein (MAb 1.1-3) (7), stripped with 0.2 M NaOH, and reprobed for detection of actin (Millipore). Protein complexes were detected

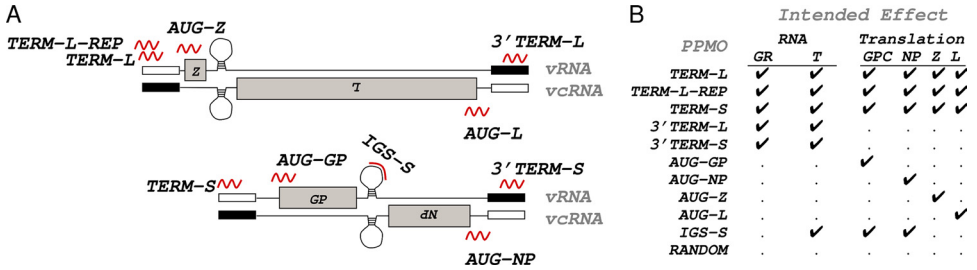

FIG. 1. Schematic representation of PPMO target sites on both arenavirus genomic RNA segments. (A) PPMO are shown in red, and genes are labeled in the 5′-to-3′ orientation. Additional potential binding sites for TERM-L, TERM-S, TERM-L-REP, 3′TERM-L, and 3′TERM-S PPMO at the viral genomic termini (black and white rectangles) are not shown on this diagram but are listed in Fig. S1 in the supplemental material. (B) Hypothetical mechanisms of action for each PPMO are indicated. Abbreviations: GR, genomic replication; T, subgenomic mRNA transcription.

using an alkaline phosphatase detection system and visualized using a Bio-Rad ChemiDoc XRS system.

Viral RNA quantitation with qRT-PCR and a GAPDH control method. Total RNA was extracted at 24 h postinfection using TRIzol per the manufacturer's protocol (Invitrogen). RNA samples were treated with DNase I (New England BioLabs) according to the manufacturer's protocol. cDNA synthesis was performed using a GoScript reverse transcription (RT) system (Promega) and LCMV Armstrong NP-specific or monkey GAPDH (glyceraldehyde-3-phosphate dehydrogenase)-specific forward primers (NP forward primer, CGAAGC TTCCCTGGTCATTTC; NP reverse primer, CAGTTATAGGTGCTCTTC CGC; GAPDH forward primer, AGTCAACGGATTTGTCGTA; GAPDH reverse primer, GGGTGGAATCATACTGGAAC). Cercopithecus-specific GAPDH primers for use with Vero-E6 cells were modified from published primers (14). Quantitative RT-PCR (qRT-PCR) was performed using an Applied Biosystems 7300 real-time PCR system platform with 250 ng of template cDNA, 12.5 μl of 2× Maxima SYBR green-ROX qPCR master mix (Fermentas), and 0.2 μM (each) forward and reverse gene-specific primers in 25-μl reaction volumes. Melt curve analysis was performed to confirm PCR product specificity. qRT-PCR analysis was performed by the comparative threshold cycle (C_T) method (28). The fold change (FC) in NP cDNA expression relative to that of the GAPDH control was determined using the equation FC = $-2^{\Delta}C_T$ (where $^{\Delta}C_T$ = NP C_T − GAPDH C_T) for infections with PPMO treatment − (C_T NP − C_T GAPDH) for infections without PPMO treatment.

***In vivo* antiviral efficacy testing.** Mice were administered 16 or 24 nmol (equivalent to ~6 or 9 mg/kg, respectively) of PPMO in water or sterile saline solution via intraperitoneal (i.p.) injection at 3 h before i.p. inoculation with 1,000 PFU of LCMV Arm53b. Similar PPMO or saline solution treatments were repeated every 24 h for 3 days. Samples of liver and spleen were collected at 4 days after inoculation, weighed, and then homogenized in phosphate-buffered saline to release virus. Tissue homogenates were subjected to titration by plaque assays as described above. Statistical analysis was performed using InStat (Graphpad, San Diego, CA).

RESULTS

PPMO design. PPMO were designed based on the Candid#1 vaccine strain of JUNV. All PPMO sequences and their arenavirus genomic complements are presented in Table 1. TERM-L and TERM-S were designed to differ slightly to permit exploration of small differences between the termini of the JUNV L and S RNA segments. TERM-L-REP includes an additional nucleotide in order to hybridize more efficiently with the nontemplated residues that are commonly found at the 5′ ends of some intracellular viral RNA species (5, 11, 12, 25). Five TERM PPMO were designed to disrupt interactions at the various genomic termini, but only TERM-L-REP, TERM-L, and TERM-S targeted the 5′ terminus of viral mRNA species and were therefore potentially more capable of interference with preinitiation events in the translation process than were the other PPMO in this study. Four PPMO (AUG-GP, AUG-NP, AUG-Z, and AUG-L) were specific to the translation initiation sites for the four JUNV mRNAs. One additional PPMO, complementary to the loop region of the intergenic transcription terminator (IGS-S), was designed to potentially interfere with viral transcription. A negative-control PPMO (RANDOM) (identical to DSCR in reference 20) that was not complementary to JUNV was used to control for non-sequence-specific effects of the PPMO chemistry. Detailed PPMO complementarity information is given in Fig. S1 in the supplemental material. PPMO binding sites are presented schematically in Fig. 1A, and the hypothetical antiviral mechanism(s) of each PPMO is given in Fig. 1B.

PPMO cytotoxicity. To determine the maximum concentration of PPMO that could be used in antiviral cell culture experiments without incurring loss of cell viability, we performed MTT cytotoxicity assays. After 24 h of treatment, TERM-L-REP, TERM-L, and TERM-S PPMO showed a low impact on viability at concentrations of up to 20 μM and mild toxicity at 50 μM in Vero-E6 cells (Fig. 2A). Prolonged incubation with PPMO (for 96 h) produced slightly stronger toxic effects (Fig. 2B). Similar results were obtained previously for PPMO in Vero or Vero-E6 cells (10, 20, 29).

Antiviral PPMO assays in cell culture. Our stock of JUNV Candid#1 grew relatively poorly in Vero-E6 cells. We sequenced the S segment of our JUNV Candid#1 strain, which

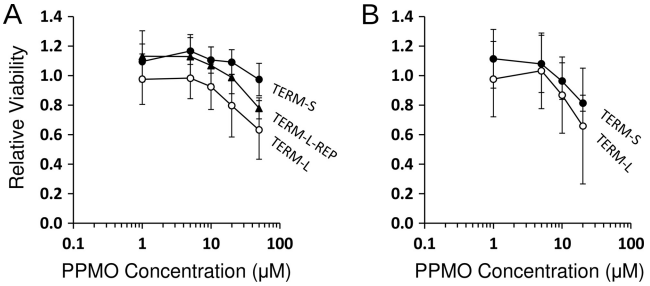

FIG. 2. Effect of PPMO on Vero E6 cell viability. MTT cytotoxicity assays were performed using uninfected Vero E6 cells incubated for 24 h (A) or 96 h (B) with increasing concentrations of the indicated PPMO before incubation with MTT. After MTT treatment for 40 min, cells were solubilized with DMSO and insoluble compound formation levels were determined photometrically at 560 nm. Viability is charted relative to mock-treated cell results (set at 1.0). Error bars denote standard deviations calculated from the results of three replicate assays.

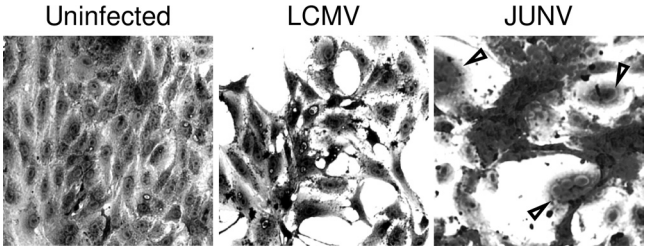

FIG. 3. Effect of arenaviruses on cellular adhesion and morphology. Cells that remained adherent after three saline solution washes and crystal violet staining are shown to illustrate changes in cellular adherence 48 h after mock infection (left panel) or infection with LCMV (middle panel). An example of cell fusion induced by modified JUNV is shown in the right panel. Arrowheads point to clusters of nuclei in the center of each syncytium.

was found to match GenBank accession number AY746353. To facilitate antiviral testing, we selected a more rapidly growing variant of JUNV Candid#1 produced by serial passage every 24 h, instead of the more usual 48 to 72 h, in Vero-E6 cells. After 17 passages, nucleotide sequencing results showed a mixture of wild-type sequence and mutant sequence, including a guanosine-to-adenosine change at position 590 (based on the numbering of AY746353). After passage 20, virus was cultured from individual plaques and sequenced again. The passage 20 virus showed a homogeneous G590A sequence. This mutation encodes a change of alanine to threonine that introduces a potential N-linked glycosylation site at amino acid 168 of GPC, which is in the GP1 region. The mechanism by which the G590A change increases viral output is not clear. The virus from passage 20 grew to a ~100-fold-higher titer and induced cell fusion at neutral pH (Fig. 3), unlike the parental strain (data not shown).

We next evaluated the effectiveness of PPMO in protecting Vero-E6 cells from JUNV-mediated cell fusion and the cytopathic effects, such as rounding and detachment from the culture flask, that are the basis of the arenavirus plaque assay. Images of Vero-E6 cell monolayers 96 h after inoculation with LCMV, JUNV, or mock inoculation are shown in Fig. 3. Long-term TCRV infection, PICV infection, and PPMO cytotoxicity (not shown) produced cytopathic effects similar to those seen with long-term LCMV infection. To assess the effectiveness of PPMO in preventing changes in cell adherence and morphology, cells were pretreated with PPMO for 3 h before inoculation at a low multiplicity of infection was performed. Morphology and adherence were evaluated 4 days after inoculation, when the virus titer typically peaks at between 10^6 and 10^8 PFU/ml. PPMO complementary to the 5′ terminus of the viral genomic RNA provided the highest overall protection against cytopathic effects caused by all four arenaviruses (Table 2). As shown by the results of the assay, TERM-S PPMO was more consistently protective than TERM-L or TERM-L-REP, perhaps due to lower cytotoxicity (Fig. 2). JUNV-specific AUG-GP, AUG-L, and AUG-Z PPMO provided less protection against JUNV and did not protect against heterologous arenaviruses. The difference in the effectiveness of terminus- versus AUG-binding PPMO was most striking in the JUNV experiment, where PPMO directed at translation of GPC and NP did not significantly reduce virus-mediated cell fusion but TERM-L, TERM-L-REP, and TERM-S PPMO treatment did. Randomized control, JUNV-specific IGS, and AUG-NP PPMO and both pan-arenavirus 3′TERM PPMO were ineffective against all viruses.

We also compared the growth characteristics of four arenaviruses in cells that were treated with PPMO for 3 h before inoculation. As in the cytoprotection assay described above, all three PPMO targeted to the genomic 5′ terminus were highly effective against each arenavirus, AUG PPMO showed moderate JUNV-specific effects, and all other PPMO were ineffective (Table 3). The levels of efficacy of TERM-L and TERM-L-REP PPMO were similar at the 20 μM treatment dose (Table 3), and for LCMV, the two PPMO were similarly effective over a 20-fold dosage range (Fig. 4).

Extensive complementarity between a PPMO and its target

TABLE 2. Quantitation of the effects of PPMO on changes in cellular adherence and morphology in arenavirus-infected cells[a]

PPMO	I[b]	JUNV		TCRV (% adherent)	PICV (% adherent)	LCMV (% adherent)
		% adherent	% nuclei in syncytia			
Untreated	−	100 ± 13	0 ± 0	100 ± 13	100 ± 13	100 ± 8
Untreated	+	64 ± 11	16 ± 5	50 ± 19	54 ± 8	46 ± 7
TERM-L	+	108 ± 7	0 ± 0	115 ± 17	83 ± 14	53 ± 17
TERM-L-REP	+	97 ± 12	1 ± 2	108 ± 8	55 ± 9	71 ± 19
TERM-S	+	114 ± 16	1 ± 1	108 ± 12	100 ± 18	100 ± 17
3′TERM-L	+	nt[c]	nt	nt	nt	1 ± 2
3′TERM-S	+	nt	nt	nt	nt	90 ± 18
AUG-GP	+	56 ± 28	11 ± 8	47 ± 21	42 ± 7	48 ± 14
AUG-NP	+	nt	nt	nt	nt	78 ± 19
AUG-Z	+	99 ± 21	9 ± 3	53 ± 13	49 ± 7	34 ± 14
AUG-L	+	nt	nt	nt	nt	48 ± 17
IGS-S	+	nt	nt	nt	nt	62 ± 14
RANDOM	+	47 ± 23	15 ± 16	62 ± 17	55 ± 6	60 ± 22

[a] Vero-E6 cells were pretreated with 20 μM PPMO for 3h, inoculated at a low multiplicity of infection in the presence of PPMO, rinsed with saline solution to remove the inoculum, and maintained in medium containing PPMO. Data represent mean numbers ± standard deviations of the results determined for adherent cells per microscope field from four representative image fields, expressed as a percentage relative to the mean of uninfected untreated control culture results.

[b] I, infected.

[c] nt, not tested.

TABLE 3. Effects of 20 μM PPMO treatment on virus titer[a]

PPMO	JUNV	PICV	TCRV	LCMV
Untreated	0 ± 0.11	0.00 ± 0.12	0.00 ± 0.06	0.00 ± 0.07
TERM-L	3.50 ± 0.08	6.42 ± 0.11	>6.9	2.46 ± 0.20
TERM-L-REP	2.09 ± 0.03	6.47 ± 0.19	>6.9	4.38 ± 0.18
TERM-S	2.16 ± 0.14	6.13 ± 0.20	>6.9	3.00 ± 0.04
3′TERM-L	−0.07 ± 0.14	nt[b]	nt	nt
3′TERM-S	−0.23 ± 0.03	nt	nt	nt
AUG-GP	0.70 ± 0.04	−0.10 ± 0.04	−0.14 ± 0.03	−0.35 ± 0.03
AUG-NP	nt	nt	nt	nt
AUG-Z	0.97 ± 0.08	0.05 ± 0.07	−0.27 ± 0.04	−0.38 ± 0.05
AUG-L	0.93 ± 0.18	nt	nt	−0.29 ± 0.01
IGS-S	−0.75 ± 0.09	nt	nt	0.23 ± 0.07
RANDOM	−0.87 ± 0.08	−0.05 ± 0.07	−0.10 ± 0.02	−0.33 ± 0.03

[a] Cells were treated with PPMO for 3h before inoculation at a low multiplicity of infection. Data represent log decreases in virus titer relative to untreated control results at 48 h after inoculation ± standard deviations. Negative values indicate that the titer increased following treatment.
[b] nt, not tested.

sequence was necessary but not sufficient for antiviral activity. All highly effective PPMO in our cell culture studies had at least 19 contiguous nucleotide matches with at least one target site on the vRNA or vcRNA of one genomic segment. However, the less effective AUG PPMO and the ineffective IGS and the 3′TERM PPMO also contained no mismatches with JUNV RNA, highlighting the importance of target site selection for PPMO efficacy (see Fig. S1 in the supplemental material). Several ineffective PPMO increased viral titers slightly (Table 3). These results suggest that, while antisense PPMO may inhibit virus growth, treatment with ineffective PPMO may enhance virus growth, as reported previously (2, 8, 20, 22).

PPMO inhibition of viral protein synthesis. To investigate the mechanism(s) of PPMO antiviral effects, we analyzed the expression of LCMV GP-C and NP in cells treated with PPMO before infection. Treatment with 2 μM TERM-L or TERM-L-REP PPMO reduced expression of viral proteins NP and GP to below the threshold of detection (Fig. 5A to D) and also reduced LCMV growth by ~1,000-fold (Fig. 4). The highest PPMO concentrations tested also decreased the expression of actin. These experiments demonstrate that PPMO complementary to the genomic 5′ terminus specifically reduced viral protein expression but also that the selectivity window between effective and cytotoxic concentrations is not wide.

To determine whether PPMO-mediated inhibition of viral protein expression could also be observed when using a multiplicity of infection higher than the 1 PFU/cell used in the experiment shown in Fig. 5A to D, cells were treated with the same PPMO concentrations as shown in Fig. 5A to D and inoculated at 5 PFU per cell. All inoculation doses tested resulted in the same pattern of inhibition of viral protein expression as seen in cells inoculated with 1 PFU/cell (data not shown), indicating that low micromolar doses of PPMO were able to suppress the growth of high multiplicities of virus.

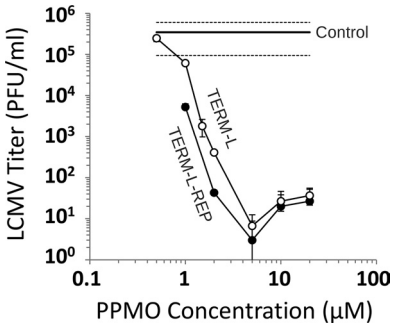

FIG. 4. Antiviral effects of PPMO treatment in cell culture. Dose-inhibition curves for LCMV-infected cultures treated with the indicated PPMO are shown. Error bars indicate standard deviations for the results from three replicate samples.

To investigate mechanism(s) of antiviral action, we next measured the effects of an effective PPMO (TERM-L) on NP RNA and protein levels. PPMO treatment caused a dose-dependent reduction in intracellular RNA levels, as shown by the use of a qRT-PCR methodology that would detect positive-sense NP from mRNA and vcRNA, and appeared to inhibit RNA accumulation more than protein accumulation (Fig. 5E to G). After 24 h of treatment with 1 μM TERM-L, NP RNA levels were reduced 10-fold while protein levels were reduced only 2-fold (Fig. 5G).

PPMO efficacy *in vivo*. As a prelude to antiviral testing in a mouse model of arenavirus infection, a PPMO dose equivalent to approximately 9 mg/kg was administered intraperitoneally to uninfected mice once per day for 7 consecutive days. The amount of PPMO used for treatment *in vivo* was based on published studies of PPMO efficacy and toxicity in mice after i.p. administration (8, 9, 32, 33). After five treatments, mice were sacrificed and the liver and kidney were examined for signs of toxicity. No gross histopathological differences between control and PPMO-treated mice were detected (data not shown), and no weight loss occurred in PPMO- or mock-treated mice.

We next evaluated the effectiveness of TERM-L, TERM-S, and TERM-L-REP PPMO during acute LCMV infection in mice. Mice were administered PPMO (~6 mg/kg/day) or sterile saline solution via i.p. injection at 3 h before i.p. inoculation with LCMV, and treatments were repeated daily for 3 days after infection. To obtain an indicator of PPMO efficacy, we evaluated viral load in the spleen and liver at 4 days postinfection. Treatment with TERM-L-REP, TERM-L, or TERM-S PPMO significantly reduced viral load per gram of tissue in both the liver and spleen compared to the combined negative control (RANDOM) and saline solution-treated con-

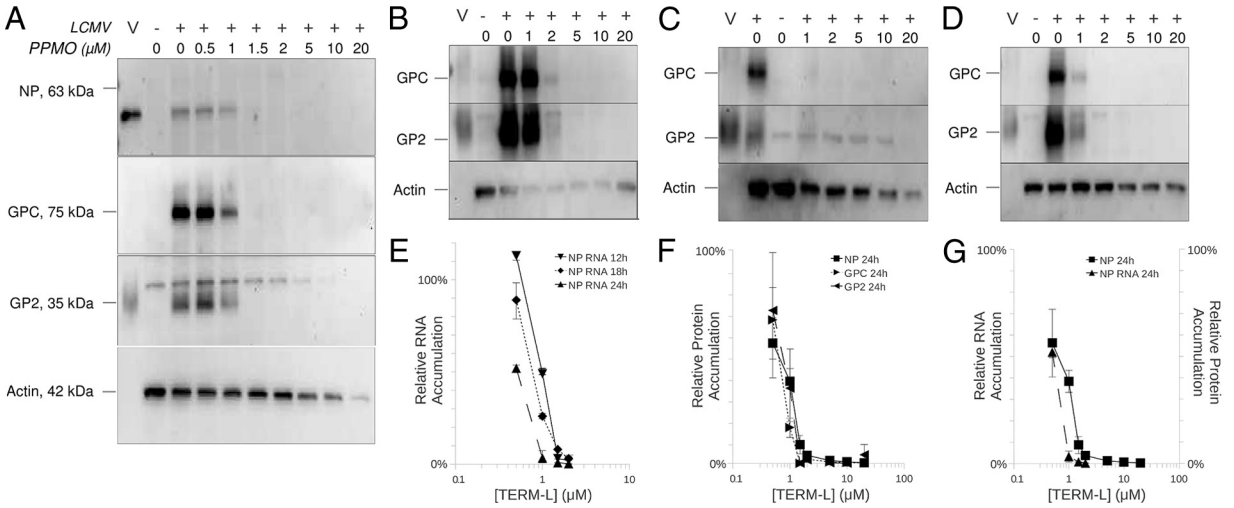

FIG. 5. Reduction of LCMV protein and RNA expression following PPMO treatment. Vero-E6 cells were pretreated with TERM-L PPMO (A and B) or TERM-L-REP PPMO (C and D) 3 h before inoculation with LCMV. Cell lysates were harvested for protein analysis 24 h (A and C) and 48 h (B and D) after inoculation. Protein from purified virions appears in the leftmost lane of each panel (V). Quantitative RT-PCR was performed to measure the amount of RNA in which the NP gene was in the positive sense, which would include both NP mRNA and S segment vcRNA. (E) Levels of NP RNA relative to GAPDH mRNA controls are expressed as percentages ± standard deviations of the results from three replicate samples relative to infected untreated control NP RNA levels 24 h after inoculation. (F) NP, GPC, and GP2 protein levels were measured by densitometry analysis of Western blots, including those shown in panel A, and are expressed as percentages ± standard errors relative to infected untreated control protein levels. Panel G compares NP and NP RNA levels 24 h after inoculation.

trol (Fig. 6A). We repeated the experiment using a higher dose (~9 mg PPMO/kg/day). The higher dose resulted in a small decrease in spleen LCMV titer, but virus titer reduction was most prominent in the liver, where titers were reduced by about 10-fold (Fig. 6B). The reduction in virus load in either the spleen or liver after large-dose TERM-L PPMO treatment was statistically significant compared to pooled saline solution and negative-control (RANDOM) PPMO treatments (analysis of variance [ANOVA]; $P < 0.05$ for spleen and $P < 0.01$ for liver). However, comparisons of high-dose TERM-L treatment to negative-control (RANDOM) PPMO treatment alone did not quite achieve statistical significance for either type of tissue. Together, these results demonstrate that short-term administration of antisense terminus-binding PPMO can reduce arenavirus growth in an animal model.

DISCUSSION

In this proof-of-concept study, PPMO complementary to the conserved 5′ termini of arenavirus genome segments were effective against a broad range of arenavirus infections in cell cultures and *in vivo* results revealed suppressed LCMV growth in the liver and spleen, the major sites of viral replication during the acute phase of LCMV infection (reviewed in reference 5). LCMV grows to high titers in mice, allowing logistically uncomplicated experimentation in the natural host animal. The disadvantage of its use is that LCMV, like all other known arenaviruses, characteristically produces only mild disease in its natural host. The pathogenesis of arenavirus hemorrhagic fevers is complex and is not fully reproduced in animal models. The results of this study represent an initial

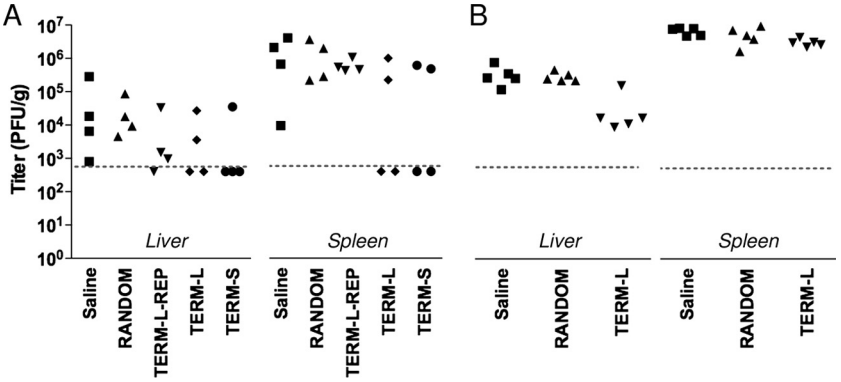

FIG. 6. Antiviral efficacy of PPMO against LCMV in mice. Mice were administered sterile saline solution or PPMO at ~6 mg/kg (A) or ~9 mg/kg (B) by intraperitoneal (i.p.) injection at 3 h before inoculation with LCMV and daily for 3 days thereafter. Tissues were collected 96 h after inoculation. Virus titers were determined by plaque assay and normalized to tissue weight. The dotted lines indicate the threshold of detection in our plaque assays.

indication of the antiviral efficacy of PPMO for an arenavirus *in vivo*. The reduction in the *in vitro* accumulation of arenavirus protein and RNA shown here suggests the activity of a mechanism whereby PPMO treatment could suppress virus growth and enable viral clearance of greater rapidity during an *in vivo* infection. However, much further investigation would be needed to determine whether PPMO could be useful in treating arenavirus infections in humans.

We tested PPMO sequences that had been designed to interfere with viral RNA synthesis or viral translation or both. The PPMO TERM, 3′TERM, and IGS-S target sites are expected to be important primarily for viral RNA synthesis, as they represent RNA that is not directly involved with translation. These three PPMO did not reduce viral titers or prevent virus-induced cytopathic effects. PPMO AUG-GP, AUG-NP, AUG-Z, and AUG-L were designed to interfere with viral translation by binding to the sequence spanning the start site of each viral open reading frame, and they also showed moderate or low activity. However, PPMO designed to target the sequence present in the 5′-terminal region of all positive-sense viral RNA species (TERM-L-REP, TERM-L, and TERM-S) and thought to participate both in translation of mRNA and in RNA synthesis events showed consistent antiviral effects in cell cultures and *in vivo*. Studies of a variety of RNA viruses have identified the 5′ genomic terminus of positive-strand RNA viruses, as well as sequences in the 5′ untranslated region (UTR) and surrounding the AUG translation start codon of viral mRNA, as frequently productive target regions for antiviral PPMO (reviewed in reference 31). In those studies, as in the present study, it was generally concluded that the most likely mechanism of action for the PPMO producing antiviral effects is through interference in events involved in the preinitiation or initiation of translation, although we cannot rule out interruption of the terminal heteroduplex or direct binding of PPMO to the L polymerase as potential antiviral mechanisms. It is not immediately clear why translation should be a process that is more susceptible to inhibition by PPMO than the interactions involved in viral RNA synthesis. Further investigation is needed to determine in more detail how the presence of a PPMO hybridized to viral mRNA inhibits events of translation.

In this study we found that, under some conditions, high doses of PPMO can produce a mildly proviral state inside the cell. PPMO-mediated enhancement of RNA virus growth has been reported previously for alphaviruses (22), coronaviruses (8, 20), and Japanese encephalitis virus (2), suggesting that this effect may be operative in RNA virus-infected cells in general. This effect may be related to the small but reproducible cell growth-enhancing effect that we observed at intermediate PPMO concentrations (Fig. 2). Further investigation is needed to improve understanding of the mechanism of PPMO-mediated enhancement of viral growth.

Treatment with small interfering RNA (siRNA) has also shown efficacy against arenavirus infection of cell cultures (3, 27), and it appears that sequence-specific approaches to arenavirus drug development may warrant further development. For PPMO, future investigation would likely include further evaluation of efficacy *in vivo* against arenaviruses of importance to public health and the generation and characterization of resistant virus, as well as efforts to improve the toxicity profile of PPMO.

ACKNOWLEDGMENTS

This work was supported by the Pacific Southwest Regional Center of Excellence for Biodefense and Emerging Infectious Diseases (AI-065359) and the California Center for Antiviral Drug Discovery (UCOP-MRPI-143226). L.H.B. was supported by the National Science Foundation (DGE-0638751).

We thank Joseph Klaus and Radin Aur for technical assistance and the Chemistry Department at AVI BioPharma, Corvallis, OR, for PPMO production.

REFERENCES

1. **Abes, S., et al.** 2006. Vectorization of morpholino oligomers by the (R-Ahx-R)4 peptide allows efficient splicing correction in the absence of endosomolytic agents. J. Control Release. **116:**304–313.
2. **Anantpadma, M., D. A. Stein, and S. Vrati.** 2010. Inhibition of Japanese encephalitis virus replication in cultured cells and mice by a peptide-conjugated morpholino oligomer. J. Antimicrob. Chemother. **65:**953–961.
3. **Artuso, M. C., P. C. Ellenberg, L. A. Scolaro, E. B. Damonte, and C. C. Garcia.** 2009. Inhibition of Junin virus replication by small interfering RNAs. Antiviral Res. **84:**31–37.
4. **Auperin, D. D., R. W. Compans, and D. H. Bishop.** 1982. Nucleotide sequence conservation at the 3′ termini of the virion RNA species of New World and Old World arenaviruses. Virology **121:**200–203.
5. **Buchmeier, M. J., J. C. de la Torre, and C. J. Peters.** 2007. *Arenaviridae*: The Viruses and Their Replication, p. 1791–1828. *In* D. M. Knipe and P. M. Howley (ed.), Fields virology, 5th ed. Lippincott Williams & Wilkins, Philadelphia, PA.
6. **Buchmeier, M. J., J. H. Elder, and M. B. Oldstone.** 1978. Protein structure of lymphocytic choriomeningitis virus: identification of the virus structural and cell associated polypeptides. Virology **89:**133–145.
7. **Buchmeier, M. J., H. A. Lewicki, O. Tomori, and M. B. Oldstone.** 1981. Monoclonal antibodies to lymphocytic choriomeningitis and pichinde viruses: generation, characterization, and cross-reactivity with other arenaviruses. Virology **113:**73–85.
8. **Burrer, R., et al.** 2007. Antiviral effects of antisense morpholino oligomers in murine coronavirus infection models. J. Virol. **81:**5637–5648.
9. **Deas, T. S., et al.** 2007. *In vitro* resistance selection and *in vivo* efficacy of morpholino oligomers against West Nile virus. Antimicrob. Agents Chemother. **51:**2470–2482.
10. **Deas, T. S., et al.** 2005. Inhibition of flavivirus infections by antisense oligomers specifically suppressing viral translation and RNA replication. J. Virol. **79:**4599–4609.
11. **Garcin, D., and D. Kolakofsky.** 1990. A novel mechanism for the initiation of Tacaribe arenavirus genome replication. J. Virol. **64:**6196–6203.
12. **Garcin, D., and D. Kolakofsky.** 1992. Tacaribe arenavirus RNA synthesis *in vitro* is primer dependent and suggests an unusual model for the initiation of genome replication. J. Virol. **66:**1370–1376.
13. **Jahrling, P. B., C. J. Peters, and E. L. Stephen.** 1984. Enhanced treatment of Lassa fever by immune plasma combined with ribavirin in cynomolgus monkeys. J. Infect. Dis. **149:**420–427.
14. **Li, X. D., H. Lankinen, N. Putkuri, O. Vapalahti, and A. Vaheri.** 2005. Tula hantavirus triggers pro-apoptotic signals of ER stress in Vero E6 cells. Virology **333:**180–189.
15. **Maiztegui, J. I., et al.** 1998. Protective efficacy of a live attenuated vaccine against Argentine hemorrhagic fever. AHF Study Group. J. Infect. Dis. **177:**277–283.
16. **McCormick, J. B.** 1986. Clinical, epidemiologic, and therapeutic aspects of Lassa fever. Med. Microbiol. Immunol. **175:**153–155.
17. **Meyer, B. J., and P. J. Southern.** 1993. Concurrent sequence analysis of 5′ and 3′ RNA termini by intramolecular circularization reveals 5′ nontemplated bases and 3′ terminal heterogeneity for lymphocytic choriomeningitis virus mRNAs. J. Virol. **67:**2621–2627.
18. **Moulton, H. M., M. H. Nelson, S. A. Hatlevig, M. T. Reddy, and P. L. Iversen.** 2004. Cellular uptake of antisense morpholino oligomers conjugated to arginine-rich peptides. Bioconjug Chem. **15:**290–299.
19. **Neuman, B. W., et al.** 2005. Complementarity in the supramolecular design of arenaviruses and retroviruses revealed by electron cryomicroscopy and image analysis. J. Virol. **79:**3822–3830.
20. **Neuman, B. W., et al.** 2005. Inhibition, escape, and attenuated growth of severe acute respiratory syndrome coronavirus treated with antisense morpholino oligomers. J. Virol. **79:**9665–9676.
21. **Ogbu, O., E. Ajuluchukwu, and C. J. Uneke.** 2007. Lassa fever in West African sub-region: an overview. J. Vector Borne Dis. **44:**1–11.
22. **Paessler, S., et al.** 2008. Inhibition of alphavirus infection in cell culture and in mice with antisense morpholino oligomers. Virology **376:**357–370.
23. **Perez, M., and J. C. de la Torre.** 2003. Characterization of the genomic promoter of the prototypic arenavirus lymphocytic choriomeningitis virus. J. Virol. **77:**1184–1194.
24. **Pinschewer, D. D., M. Perez, and J. C. de la Torre.** 2005. Dual role of the

lymphocytic choriomeningitis virus intergenic region in transcription termination and virus propagation. J. Virol. **79:**4519–4526.
25. **Polyak, S. J., S. Zheng, and D. G. Harnish.** 1995. 5′ termini of Pichinde arenavirus S RNAs and mRNAs contain nontemplated nucleotides. J. Virol. **69:**3211–3215.
26. **Raju, R., et al.** 1990. Nontemplated bases at the 5′ ends of Tacaribe virus mRNAs. Virology **174:**53–59.
27. **Sánchez, A. B., M. Perez, T. Cornu, and J. C. de la Torre.** 2005. RNA interference-mediated virus clearance from cells both acutely and chronically infected with the prototypic arenavirus lymphocytic choriomeningitis virus. J. Virol. **79:**11071–11081.
28. **Schmittgen, T. D., and K. J. Livak.** 2008. Analyzing real-time PCR data by the comparative C(T) method. Nat. Protoc. **3:**1101–1108.
29. **Sleeman, K., et al.** 2009. Inhibition of measles virus infections in cell cultures by peptide-conjugated morpholino oligomers. Virus Res. **140:**49–56.
30. **Stein, D., E. Foster, S. B. Huang, D. Weller, and J. Summerton.** 1997. A specificity comparison of four antisense types: morpholino, 2′-O-methyl RNA, DNA, and phosphorothioate DNA. Antisense Nucleic Acid Drug Dev. **7:**151–157.
31. **Stein, D. A.** 2008. Inhibition of RNA virus infections with peptide-conjugated morpholino oligomers. Curr. Pharm. Des. **14:**2619–2634.
32. **Stein, D. A., et al.** 2008. Treatment of AG129 mice with antisense morpholino oligomers increases survival time following challenge with dengue 2 virus. J. Antimicrob. Chemother. **62:**555–565.
33. **Stone, J. K., et al.** 2008. A morpholino oligomer targeting highly conserved internal ribosome entry site sequence is able to inhibit multiple species of picornavirus. Antimicrob. Agents Chemother. **52:**1970–1981. 508.
34. **Summerton, J.** 1999. Morpholino antisense oligomers: the case for an RNase H-independent structural type. Biochim. Biophys. Acta **1489:**141–158.
35. **Summerton, J., and D. Weller.** 1997. Morpholino antisense oligomers: design, preparation, and properties. Antisense Nucleic Acid Drug Dev. **7:**187–195.